INL/EXT-21-63886

Design optimization for Printed Melt Wire Arrays Encapsulation

July 2021

Lance Hone, Kiyo Fujimoto, Kory Manning, Malwina Wilding
Idaho National Laboratory

Idaho National Laboratory

INL is a U.S. Department of Energy National Laboratory
operated by Battelle Energy Alliance, LLC

INL/EXT-21-63886

Design optimization for Printed Melt Wire Arrays Encapsulation

Lance Hone, Kiyo Fujimoto, Kory Manning, Malwina Wilding
Idaho National Laboratory

July 2021

Idaho National Laboratory
Idaho Falls, Idaho 83415

http://www.inl.gov

Prepared for the
U.S. Department of Energy
Office of Nuclear Energy
Under DOE Idaho Operations Office
Contract DE-AC07-05ID14517

Page intentionally left blank

ABSTRACT

As part of the Nuclear Energy Enabling Technology (NEET) Advanced Sensor and Instrumentation (ASI) Program, Idaho National Laboratory (INL) has recently established in-house capabilities to fabricate and test new advanced-manufactured sensors for measuring peak irradiation temperature within a nuclear test reactor. Although methods of real-time temperature monitoring, such as thermocouples, may be used, the complexity of feedthroughs and attachments to collect real-time measurements greatly increases the cost of the experiment. Instead, passive monitoring techniques may be used for peak- temperature measurement that exploit the melting point of well-characterized materials (standard melt wires) to infer peak reactor temperatures. However, limited available space for instrumentation during experiments introduces an additional challenge. To accommodate this, INL has expanded its temperature- detection instrumentation capabilities to include advanced-manufactured (AM) melt wires for peak irradiation temperature measurements. These melt wires can determine peak temperatures while also accommodate space limitations in irradiation experiments. In an effort to improve performance reliability of AM melt-wire capabilities, a process was developed and tested to identify the significance of entrapping a high purity inert atmosphere within the packaging of printed melt wire arrays. The materials used in this study were aluminum, zinc, and tin encapsulated in high purity helium within a stainless steel (SS) 316 container. Tin, with a low melting point of approximately 230°C, Zn with a mid-melting point of approximately 420°C, and Al with a high melting point of approximately 660°C. This report describes the design, fabrication process, furnace testing and X-ray Computed Tomography (XCT) evaluation. Results show a successful outcome in creating an inert gas encapsulation and high-resolution evaluation methods.

ACKNOWLEDGEMENTS

This work was supported through the Nuclear Energy Enabling Technology (NEET) Advanced Sensor and Instrumentation (ASI) Program, under Department of Energy (DOE) Idaho Operations Office Contract Number DE-AC07-05ID14517. We would like to thank Robert Seifert, James Milloway, Kurt Davis, and Richard Skifton for their technical contributions in this work.

Page intentionally left blank

CONTENTS

FIGURES

Page intentionally left blank

ACRONYMS

AJP aerosol-jet printing

AM advanced manufacturing

ASI Advanced Sensor and Instrumentation

ATR Advanced Test Reactor

DOE Department of Energy

DSC differential scanning calorimetry

HTTL High Temperature Test Laboratory

IJP ink-jet printing

INL Idaho National Laboratory

MDP micro-dispense printing

MTR Material Test Reactors

NE nuclear engineering

NEET Nuclear Energy Enabling Technology

PA pneumatic atomizer

PIE post-irradiation examination

PVP polyvinylpyrrolidone

SS stainless steel

USP United States Pharmacopeia

XCT X-ray Computed Tomography

Page intentionally left blank

Design optimization for Printed Melt Wire Arrays Encapsulation

1. INTRODUCTION

Irradiation testing is used to gain insight toward a wide range of radiation-induced phenomena to understand the performance of fuels and materials in reactor environments. Recently, focus on advanced reactor fuel forms has further emphasized the need for cultivating a greater understanding of irradiation effects on fuels and materials performance requiring the development of a new approach for in-pile instrumentation [1]. For this, specialized experiments for material evaluation are key to ensure the safety and reliability of advanced reactors. A key parameter in irradiation experiments is temperature, and temperature monitoring is accomplished through both passive- and active-monitoring techniques. Active-monitoring techniques, such as thermocouples, provide real-time data and are typically expensive because of the engineering challenges to accommodate instrumentation leads. Passive-monitoring techniques are typically used in static irradiation capsules to provide insight toward peak temperatures [2]. These passive techniques are the preferred method for temperature monitoring when irradiation tests are seeking a less-expensive measurement method and/or the experiment requires instrumentation without leads, such as for static capsule experiments [3].

Melt wires are a passive monitoring technique that enable experimenters to identify the peak temperature achieved during an irradiation test [4]. This method involves placing wires that have both a known composition and a well-characterized melting temperature within an experiment or test environment. The peak temperature is then inferred during post-test examination or post-irradiation examination (PIE) when the wire is inspected for visual signs of melting. It is reasoned that the peak temperature during testing has exceeded the melting point of wire material if signs of melting are apparent. On the other hand, it is determined that the peak test temperature remained below the melting point of the wire material if the wire does not show any signs of melting. Preferably, materials for melt wires have a low neutron-absorption cross-section while exhibiting distinct and reproducible melting behavior when they have been exposed to temperatures beyond their respective melting point. Also, the potential for a combination of materials within an encapsulated melt pack to react with one another or vapor alloy from low eutectic points at high temperatures is considered.

With the development of meticulous material selection and validation procedures, the High Temperature Test Laboratory (HTTL) at Idaho National Laboratory (INL) has produced a set of methods for classical melt-wire fabrication that includes the ability to encapsulate multiple wire materials into one small-diameter unit [**Error! Reference source not found.**]. The library of qualified materials for melt-wire selection contains more than 40 useful materials with a detection range between 29.73 and 1535°C [**Error! Reference source not found.**]. While standard melt wires are commonly used in test-reactor experiments, supported by Material Test Reactors (MTR) such as the Advanced Test Reactor (ATR), sensor design constraints are related to predesigned capsules with geometries imposed by the layout of the MTR core. These capsule designs may only allow for sensors that are couple of millimeters in diameter and with pre-determined geometries. As multiple specimens are contained within the capsules at once, this can leave little or no space for instrumentation.

The production of miniature, robust sensors is possible with additive-manufacturing techniques such as aerosol-jet printing (AJP), ink-jet printing (IJP), and micro-dispense printing (MDP). The incorporation of these technologies enables the development of advanced sensors and instrumentation for reactors and fuel-cycle facilities with printing patterns as small as 10 μm. These feature sizes would be advantageous for device miniaturization, especially when considering that traditional melt-wire capsules typically require a wire length of approximately 2 mm [5]. Through the AM portion of the NEET ASI Program,

novel technologies such as AJP are being explored for the development of unique sensors that are otherwise unobtainable with conventional fabrication processes.

Previous work on the development of AM melt wires was recently reported [7,8] and include a method to miniaturize melt wire encapsulation and a benchmark study on AM melt wires using in-house synthesized inks. The first study developed a metal encapsulation method to seal and miniaturize the overall size of the melt wire array but it did not provide a way to create an inert atmosphere within the sealed capsule and was not optimized for the imaging technique selected for melt evaluation [7], [8]. The second study included benchmark testing of AM melt wires fabricated with AJP to evaluate the performance reliability of AM melt-wires when compared to standard bulk materials. To demonstrate the ability to incorporate AM techniques for the fabrication of advanced nuclear in-pile passive temperature sensors, it required a comparison between standard and AM melt wires of tin, aluminum, and zinc. To minimize the number of variables introduced during benchmark testing, the encapsulation method for both the traditional and AM melt wires was based on classical fabrication techniques that do not allow for overall device miniaturization. Benchmark testing was accomplished with differential scanning calorimetry (DSC) and furnace testing, and it was determined that the performance of the AM melt-wire capsule was consistent with that of the standard melt-wire capsule.

Recent efforts included significant improvements on the encapsulation design for AM melt wires. The most recent iteration allows for an inert atmosphere within the capsule, which is critical for melt wire performance especially when melt wire oxidation is of a concern. Also, this new design is further optimized for XCT, which is the imaging technique required to evaluate melt behavior when an opaque encapsulation material is used. To assess the necessity of having an inert atmosphere within the encapsulation a comparison of melt behavior between melt wires encapsulated in air and those in an inert atmosphere was performed. The work highlighted in this report uses the same materials as the benchmark study on AM melt wires where the low melting-point material used was Sn at approximately 230°C, mid-melting material used was Zn at approximately 420°C, and the high melting-point material used was Al at approximate melting point of 660°C to assess the new design.

2. MATERIALS AND METHODS

2.1 Melt Wire Overview

Melt wire materials are selected to provide insight towards the peak temperature achieved in a projected location of an experiment. In a typical experiment, a standard container of traditional melt wires would contain 3 materials. Each experiment has a projected peak temperature and material selection begins by identifying a material having a melting point approximately 20 to 30˚C below the expected peak temperature of an experiment. The next material selected would melt at or near the expected peak temperature, and the last material would have a melting point that exceeds the experiment's projected peak temperature by about 20 to 30˚C. Under normal experimental conditions, the last material is not expected to melt; however, if it does occur this can provide valuable information towards unforeseen events that could occur during an experiment that may otherwise have been missed. After melt wire fabrication is completed, images of the wires are obtained to serve as a reference for the post-experiment melt behavior of each melt wire.

The melt wire package used for this study is unlike a typical peak-temperature tests, as its purpose is to serve as an evaluation of AM melt wires that would span a wide range of melting temperatures. Selecting materials spanning this wide range will elucidate whether melt wire performance was affective by using AM methods for melt wire fabrication.

2.2 Encapsulation Re-Design and Sealing Process

First attempts at miniaturizing melt wire packaging included a 2 mm diameter and 0.5 mm thick Stainless Steel 316 (SS316) disk. It was milled to create a dimple or a pocket and melt wire materials that were printed within the dimple. Next, a blank SS316 wafer was placed on the printed side of the previously printed melt wire chip, and laser micro-welded to seal and encapsulate the printed materials within SS316 [8]. However, this initial design was not optimized for XCT imaging and did not provide a path forward for sealing printed melt wires within an inert atmosphere.

A second iteration of the encapsulation design was aimed towards improving upon the initial design by addressing two critical features. First, the thickness of the encapsulation material was significantly reduced to a side wall thickness of 0.6 mm and a floor thickness of 0.2 mm, as higher thickness introduces challenges in resolving the printed material by using the XCT. Minimizing the amount of encapsulation material surrounding the printed wires reduces the attenuation caused by the excess amount of encapsulation material, which ultimately enhances the ability to evaluate melt wire performance with XCT. Second, design changes and a new sealing process were introduced that would facilitate the encapsulation of the printed materials within an inert atmosphere, which is critical for the performance of oxygen sensitivity of the melt wire materials. Third, to minimize premature melting of the wires during the sealing process the printed wires were intentionally placed in the location opposite to the laser welding.

For this sealing process, changes included the design of a top lid to be attached using a precision laser welder. To aid in the laser welding process, a shoulder was built into the wall of the base to allow the lid to sit recessed in the container such that the lid and base provided a flush surface to weld on. On the center of the lid, a small extrusion (Figure 1) was added as a feature to assist with handling.

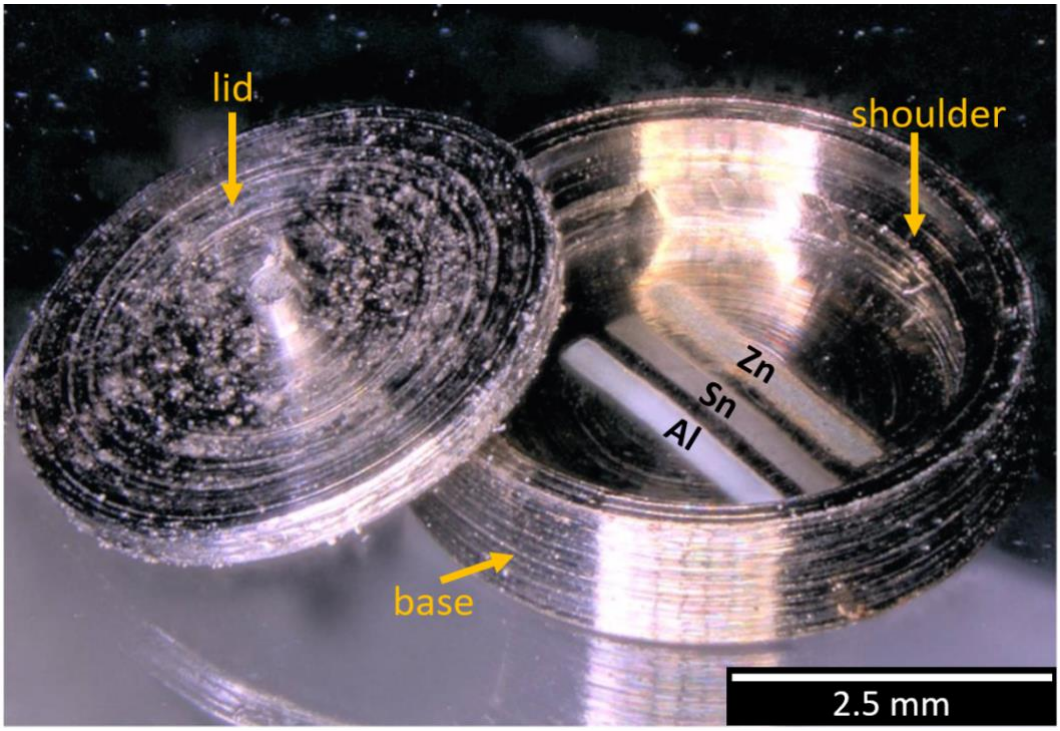

Figure 1 – Melt wire container ready to be sealed with printed melt wires on substrate.

Laser welding was accomplished with a LaserStar Fiberstar Workstation 7600, and seal welds were completed using 180 W with specific settings at 2.6 J, a pulse width of 16 ms, and a beam diameter step

of 5. To create an inert atmosphere within the encapsulation, a small weep hole was created in the lid (approximately 250 µm) prior to attaching the lid to the base, and a weld was created around the entire lid in air. While laser welding the lid, applying too much energy during the sealing process initially melted the printed melt wires with lower melting points. To prevent premature melting, it was necessary to use a copper cradle custom fit to press against the melt wire container base to be used as a heat sink capable of absorbing all excess heat generated from the laser weld. To ensure melting point temperature of the melt wires was not exceeded, temperature measurements were monitored on the prototypes by using a laser welder to attach the thermoelements (type K) directly to the heat sensitive substrate area where the printed melt wires were located. Laser welds were then performed using the energy necessary to close the lid. After a few modifications to ensure a tight fit from the copper to the container, temperatures could be limited to a maximum of 135˚C ensuring no pre-mature melting of the melt wire materials. (Figure 2)

Next, an inert atmosphere was introduced into the sealed container by suspending it within a vacuum system to purge all air and was backfilled with high purity helium. The final seal was completed by shooting the laser through a quartz window while the melt wire container is in view within the vacuum system as seen in Figure 2.

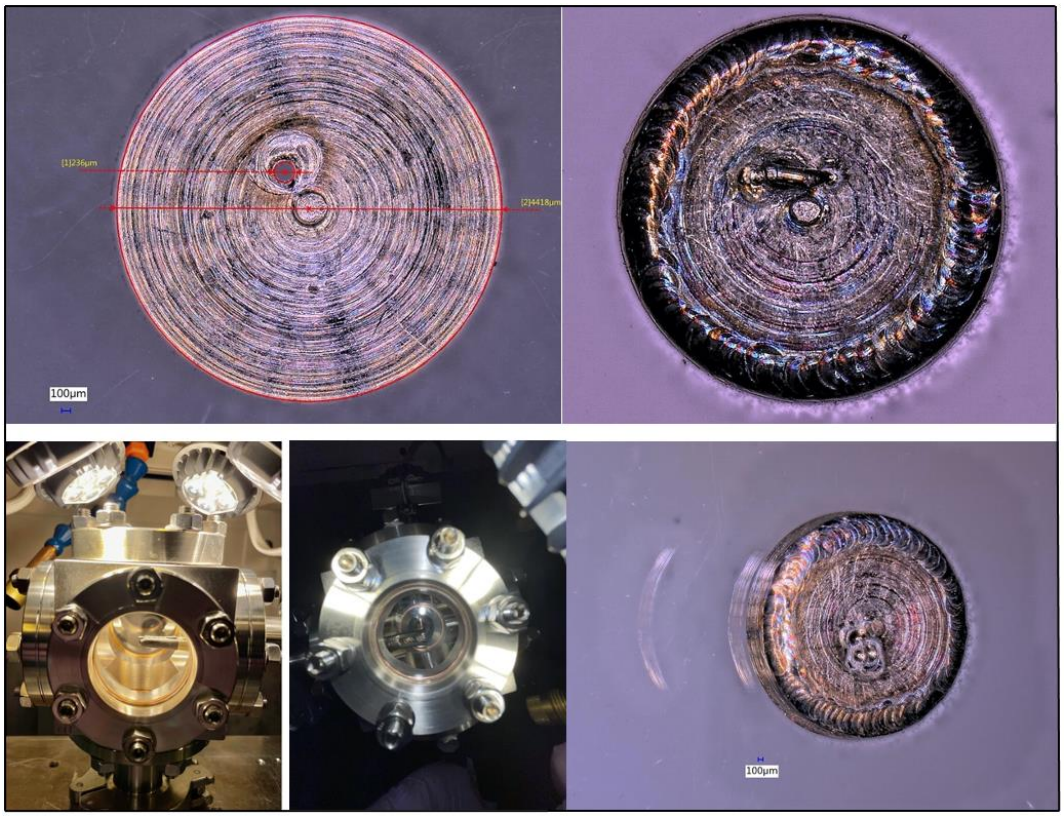

Figure 2 - Top Left: Melt wire container with ~250µm hole created by laser. Top Right: Melt wire container prepared with wire across weep hole for welding. Bottom Left: Vacuum chamber to encapsulate helium into melt wire container. Bottom Middle: Looking down from laser head at sample suspended within the vacuum chamber. Bottom Right: Micrograph of a completed helium encapsulated container.

To ensure that an inert atmosphere was maintained within the container, the sealed piece was subjected to a helium leak check to confirm that a true seal exists. Following this, an initial XCT image was obtained as a reference image that compared to a final XCT image obtained to identify if whether melting has occurred. Detailed images of this are shown and discussed in the EVALUATION section of this report.

3. FABRICATION

3.1 Printed Melt Wires

The incorporation of advanced fabrication methods for the preparation of melt wires required the development of ink materials containing the desired melt wire materials while also being compatible with additive printing technologies. For this study, AJP compatible inks were synthesized that contained the melt wire materials of interest and were purchased as nanopowders. Aluminum nanopowder (99.9%, 800 nm, PVP coated), zinc nanopowder (99.9%, 95-105 nm, PVP coated) and tint nanopowder (99.9%, 60-80 nm, PVP coated) were all acquired commercially from US Research Nanomaterials (Houston, Texas). Nanopowder dispersion were achieved with the use of 200 proof ethanol (USP grade, Fisher Scientific), ethylene glycol (high purity, VWR Life Science), and BYK-156 (BYK USA Inc.). All chemicals and reagents were used as received without further purification or modification.

First, a stock solution was created to act as the dispersion medium for the nanopowders and was composed of 0.1 g of BYK-156 added to a 1:3 solution of ethanol to ethylene glycol, which was allowed to stir for one hour. Three different AJP inks were created from each individual nanopowder. For the optimization process, inks having a nanopowder loading of 60 wt% were initially produced utilizing a high shear mixer (5000 RPM for 15 minutes; L5M-A equipped with a 5/8" micro tubular mixing unit, Silverson). To benchmark the performance of the initial ink composition, AJP was utilized, and, depending on the consistency of the output, additional solvent was added. If necessary, the dispersion medium was added in 5 mL increments, and then subjected to high shear mixing. This process continued until the desired output and ink performance was achieved. Final concentrations for each of the inks are as follow: 45 wt%, 60 wt % and 40 wt% for tin, aluminum, and zinc, respectively.

Printing was achieved with the pneumatic atomizer (PA) of an Optomec Aerosol Jet 200 equipped with a 200 µm nozzle. The bubbler solvent add-back system having a 1:1 ratio of ethylene glycol to ethanol was utilized to minimize the effects of solvent loss during atomization. During printing, the ink was held at 35 °C to optimize ink atomization. The tool platen temperature (65 °C), pneumatic atomizer (600 CCM), virtual impactor (500 CCM), and sheath gas (50 CCM) flow rates were optimized to ensure line widths and material deposition of functional materials were adequate to obtain the desired device dimensions. SS 316 was utilized as the substrate for the printed melt wires. Prior to printing, the substrates were triple rinsed (acetone, methanol and nanopure water) within an ultrasonic bath to clean the substrate surface. After each subsequent cleaning, nitrogen gas was used to dry the substrate.

3.2 X-Ray Computed Tomography (XCT)

SS316 was chosen as the encapsulation material primarily for its capability for print adhesion, machinability, and weldability. Using SS316 as the encapsulation material eliminated the ability to use the traditional method of visual observation for evaluating melt behavior of AM melt wires. To overcome this, XCT was used to produce detailed images of the melt wires before and after furnace tests. Since different materials have different melting characteristics, it is important to identify features which result from melting such as rounded edges where sharp features had previously existed, the formation of a sphere of the entire melted line, or the development of bubbles or beads while the bulk of the material appears unaffected. From Figure 3, the XCT images obtained from these experiments were able to provide accurate measurements of details as low as 50 µm with a software capable of measuring features as small as 4 µm. This provided extreme improvement in identifying unique melting characteristics each material may have. It is important to note that the melt wire evaluation method discussed in this report is the same method that would be used to evaluate these containers for PIE.

Evaluation of melt wires is accomplished by obtaining initial XCT images of a sealed melt wire assembly before the experiment to serve as a reference point. Then, after the experiment a new XCT image is obtained and compared against the reference image to determine if any changes had occurred. Part of the fabrication process is to test prototypes of each material using the same imaging techniques used for PIE to identify any characteristics that indicate melting has occurred.

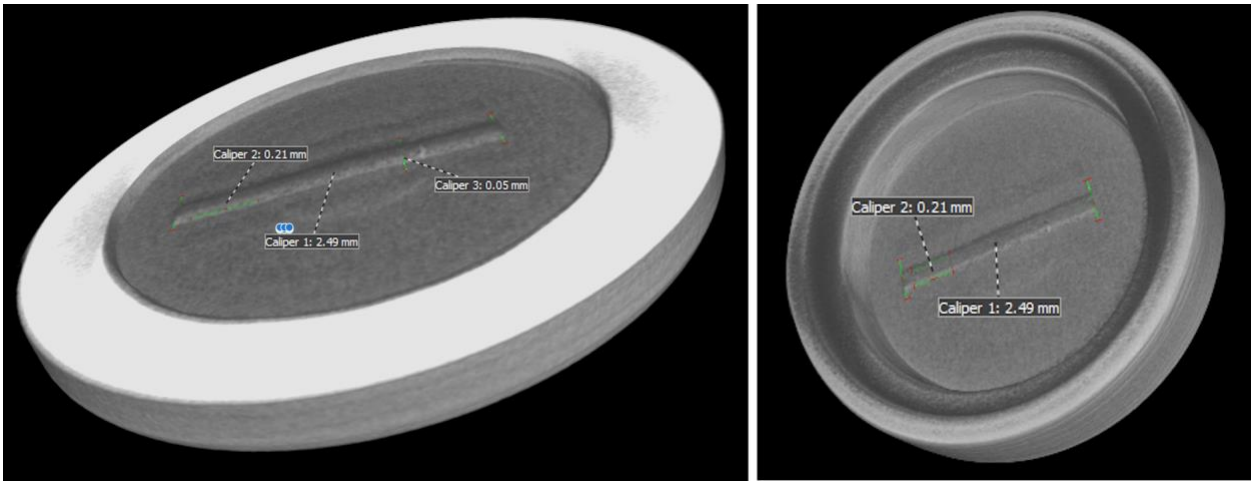

Figure 3 - A demonstration of the capability XCT imaging to examine the melt wire containers at different orientations and provide accurate measurements as small as 50 µm.

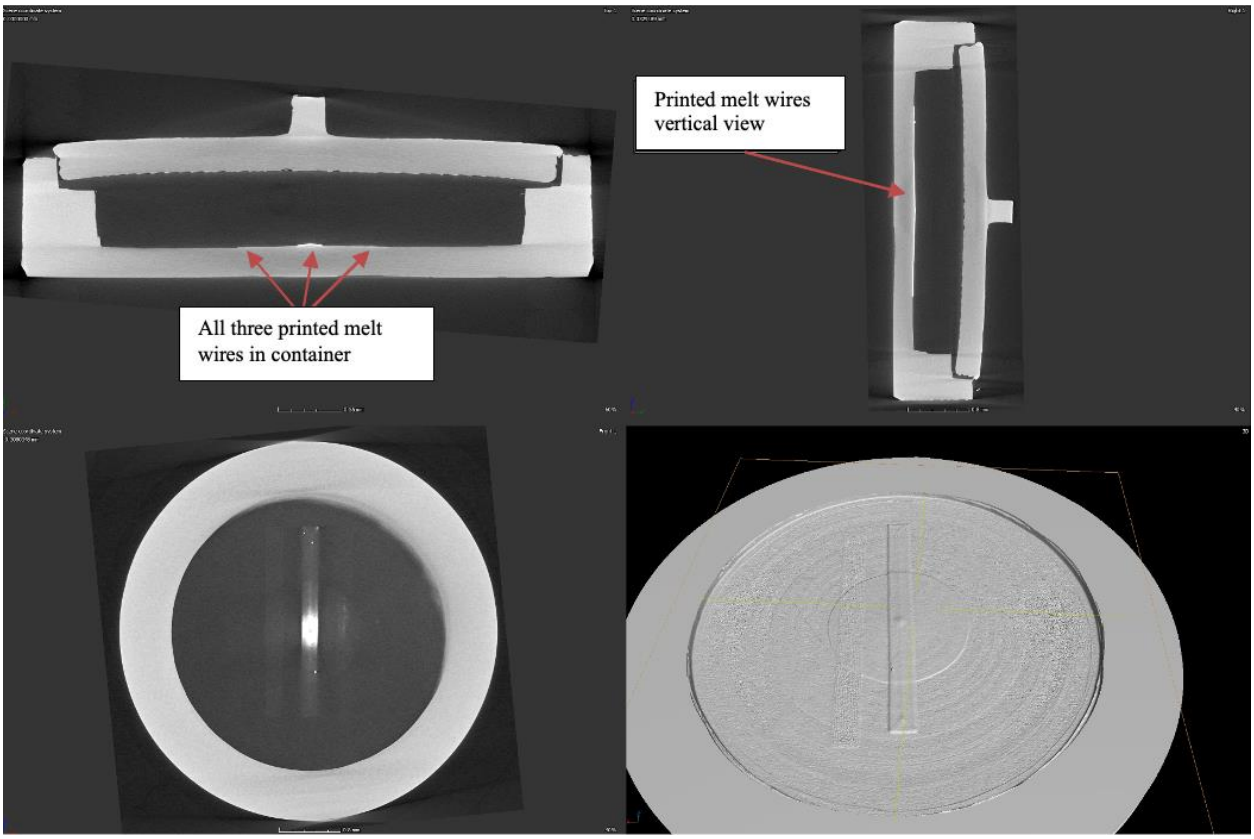

Figure 4 - A typical set of XCT images as seen when evaluating an encapsulated array of printed melt wires. This container has not been seal welded. Top Left: Horizontal cross section of container. Top Right: Vertical cross section of container with melt wires turned vertical. Bottom Left: Top view of container looking past lid. Bottom Right: Isometric view of container (Left to right: Zn, Sn, Al).

4. EVALUATION

Melt wire performance tests were completed with assemblies containing helium gas to evaluate the impact of the environment. Initial considerations towards melt wire containment did not entrap an inert atmosphere to ensure good melt wire performance because of the use of silver in initial evaluations, and oxidation was not of a significant concern [8]. However, most materials used to fabricate melt wires were prone to oxidation, and to support the use of these materials in an inert atmosphere is critical.

To demonstrate the need for an inert atmosphere for all the oxidation sensitive materials, a melt wire assembly was assessed having an air encapsulation. A reference XCT image was collected before the melt wires were exposed to a temperature above their expected melting point. Those samples with an air encapsulation did not show distinguishable signs of melting even after exceeding expected melting temperatures more than 50˚C. However, aluminum melt wire did exhibit some unexpected behavior when exposed to temperatures beyond its expected melting temperature in that the line detached from the SS316 substrate and started bending upward. This uncharacteristic phenomenon can be observed in Figure 5, but this was only after reaching a temperature well in-excess (greater than 50˚C) of its expected melting point of 660˚C.

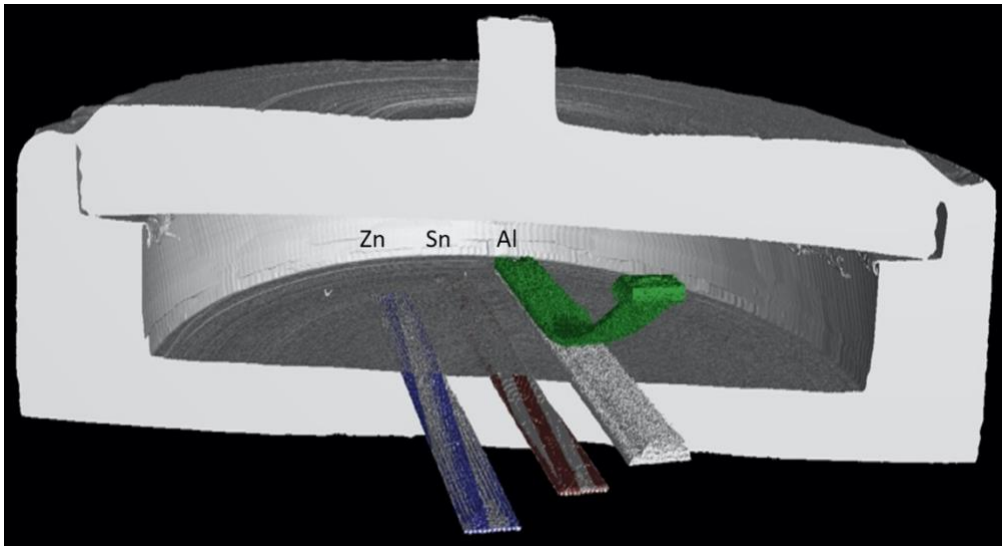

Figure 5 - Cross section of a post furnace XCT image superimposed over pre-furnaced image of a container sealed in air. Melt wires without color were taken before the furnace test. Melt wires with color were taken after exceeding the melting point of all 3 materials indicating no visible changes on 2 out of 3 wires when encapsulated in air.

To compare melt wires in an air environment to the performance of the melt wires in an inert gas environment, the same printed materials in an identical container to the one used for the test in air were used. The open container was placed in a quartz tube and air was evacuated and refilled with helium using a vacuum system. The tube was then sealed and placed in a furnace to be exposed to temperature above the melting point of tin. As seen in Figure 6, the micrograph of the open container shows the typical bead formation as melting characteristic of tin when compared to previous experiments evaluating tin printed lines. Furthermore, XCT images were taken of the open container to confirm the bead formations were recognizable in both viewing methods. This comparison of air to inert gas environments demonstrates the significance of inert atmosphere encapsulation to rely on the material to perform as expected.

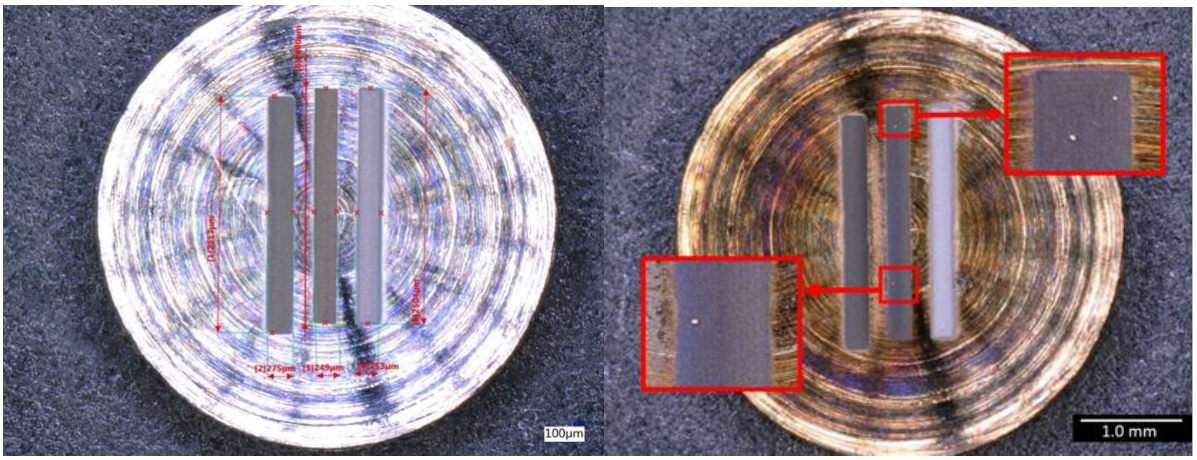

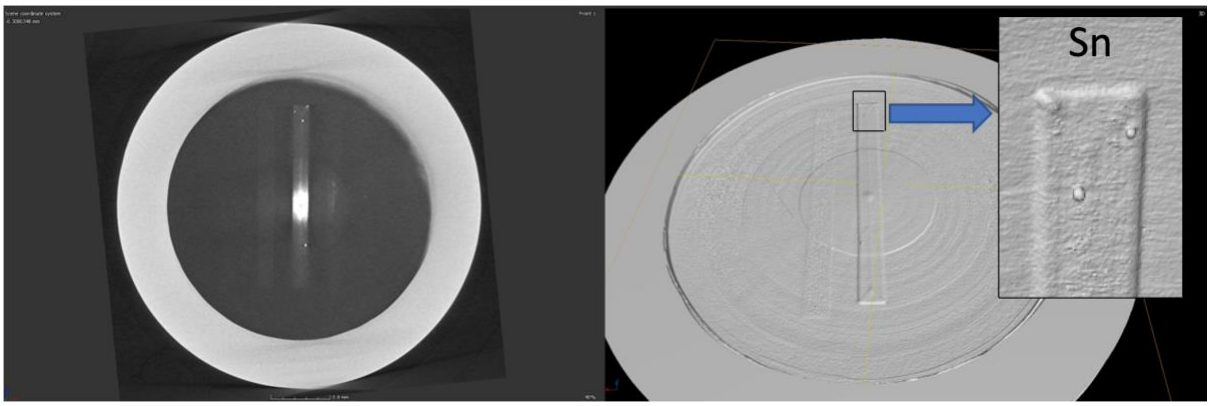

Figure 6 - Images of melt. Top Left: Micrograph with of the pre-furnaced open container. Top Right: Micrograph highlighting bead formation on center tin wire. Taken after exceeding the melting point of tin in an open container and an inert atmosphere tube. Bottom Left: Top view of XCT image showing bead formations. Bottom Right: XCT image of open container showing the same bead formations.

Finally, a melt wire assembly having an inert encapsulation was evaluated using XCT. Like the air encapsulation, a reference XCT image was collected before the melt wires were exposed to a temperature above their expected melting point. The assembly was then exposed to a temperature exceeding the melting point of all three materials (680˚C). XCT images were then taken to evaluate the changes that should have occurred from melting. Contrast levels were adjusted for each melted material to provide the most details for each image. Scans were performed at a 4 µm resolution with contrast levels as low as 50:1. (Figure 7 & Figure 8)

As previously discussed, melting is determined when changes can be identified between XCT images before exposure to melting temperatures when compared to images obtained after. The initial XCT image in Figure 7 is a top view using an average contrast capable of showing all 3 materials in the container. Although the image is not clear for specific single material, all materials can be identified within the container. This image also showed unexpected features in the printed lines that likely occurred due to weld spatter during the final laser weld for sealing the inert gas into the container. Steel spheres are shown in this image that are also speculated to be from the final weld. These recognizable features were advantageously used to aid in aligning the container to help with the post-furnace comparison.

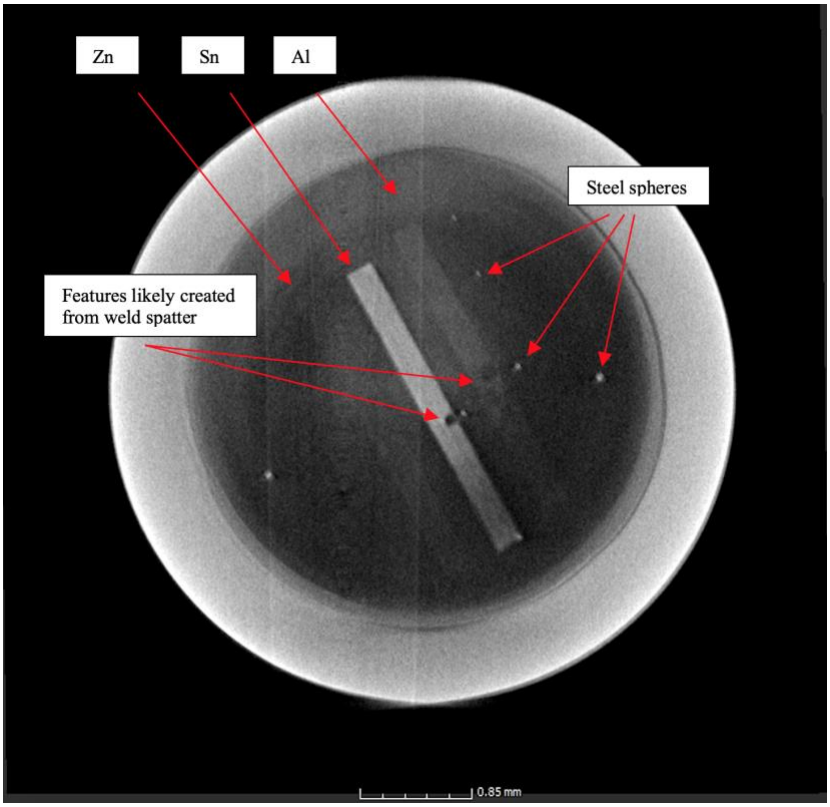

Figure 7 - Top view of an initial XCT with average contrast showing all 3 melt wires. Features in melt wires were likely caused from weld spatter.

Tin was the lowest melting point material and had the most obvious changes compared to the other two printed materials. From Figure 8 the tin collected in a pool near the center of the container. Initially this image was difficult to locate due to its new shape however, using the identifying feature likely caused from the weld sputter assisted in aligning the container and confirming this was tin. The post furnace image was enhanced with color to help with the inspection.

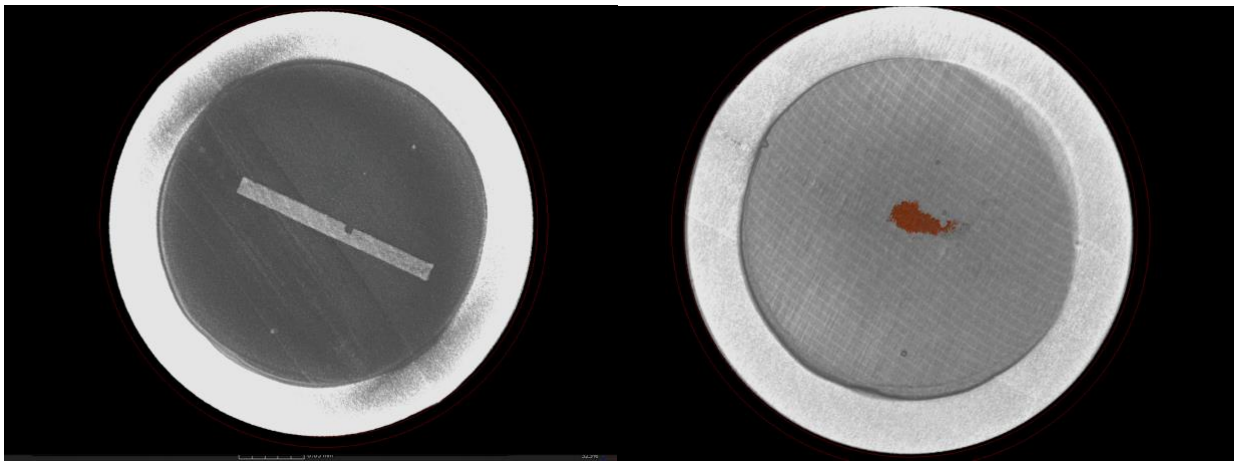

Figure 8 - XCT images of tin before and after exceeding the melting temperature using feature to confirm the material. Left: Original XCT image of tin encapsulated in helium. Right: Post-furnace image of melted tin enhanced with color.

The XCT images of the zinc melt wire were not clearly defined. However, after adjusting contrast to optimize the XCT images, subtle changes could be identified to imply melting had occurred. In Figure 9 it can be observed that when compared to the original XCT image, a section along the wire showed new separated areas signifying melting characteristics observed in previous tests where the zinc wire appears to fade along the original printed line and collect in new areas. It may be worth noting that the zinc images show some lines and features that do not actually exist. These are artifacts created from motions of tooling components or objects during XCT image acquisitioning that can be ignored during evaluation.

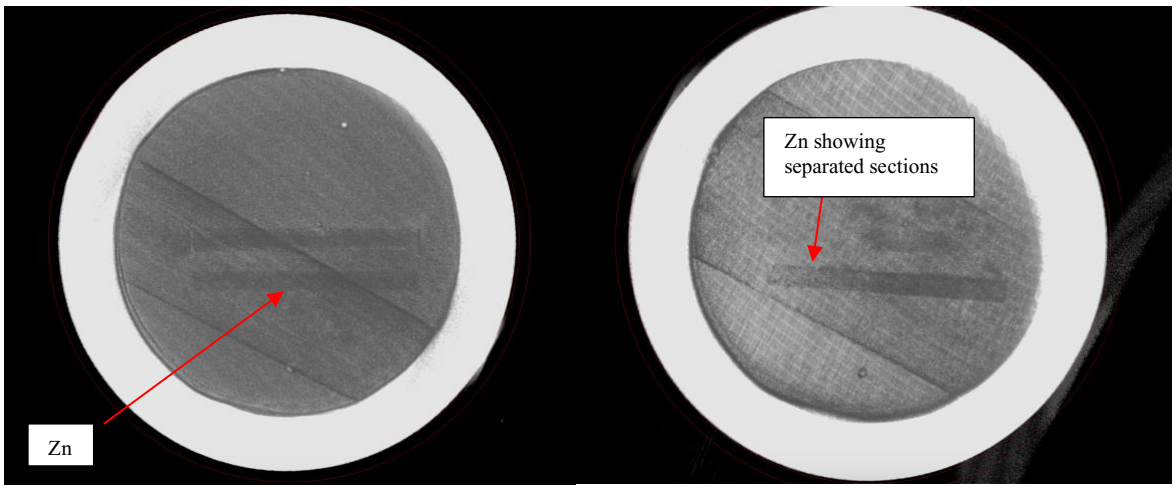

Figure 9 - Left: Original XCT image of zinc. Right: Post-furnace zinc image showing separated sections indicating melt. Artifacts in the background can be ignored.

For the evaluation of aluminum, the printed line on the original XCT image was unclear, and in the post-furnace image the aluminum wire was even harder to identify. It was unclear as to whether it had melted, relocated or was just unidentifiable against the substrate. Therefore, confirmation of melting was considered inconclusive. It was determined that the combination of aluminum and stainless steel do not perform well together due to a low contrast between them. Low contrast occurs from the similarity in certain material properties, which would require further investigation for compatible substrate and melt wires combinations.

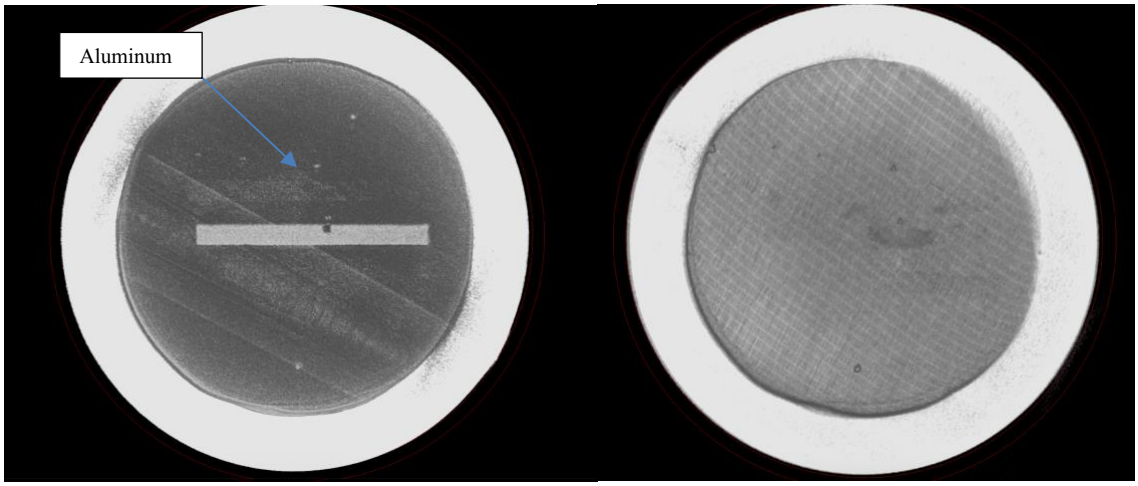

Figure 10 - Left: XCT original image with custom contrast to identify aluminum printed wire. Right: Post-furnace XCT image showing inability to locate aluminum wire.

5. CONCLUSION

As part of the NEET ASI Program, INL has demonstrated design optimization for AM melt wire encapsulation. To improve performance reliability of AM melt-wire capabilities, a process was developed and tested to identify the significance of entrapping a high purity inert atmosphere within the packaging of printed melt wire arrays. The materials used in this study were aluminum, zinc, and tin encapsulated within a SS316 container. SS316 was chosen as the encapsulation material primarily for its capability for print adhesion, machinability, and weldability. Tin, with a low melting point of approximately 230°C, Zn with a mid-melting point of approximately 420°C, and Al with a high melting point of approximately 660°C were chosen for a wider melting point range. Encapsulation design was aimed towards improving upon the initial design, where the thickness of the encapsulation material was significantly reduced that ultimately enhanced the ability to evaluate melt wire performance with XCT. The initial melt wires that were sealed in an air encapsulation did not show distinguishable signs of melting even after exceeding expected melting temperatures more than 50˚C; therefore, additional design changes and a new sealing process were introduced. Both changes facilitated the encapsulation of the printed materials within an inert atmosphere, which is critical for the performance of oxygen sensitivity of the melt wire materials. During the inert gas encapsulation process it was important to minimize premature melting of the wires thus the printed melt wires were intentionally placed in the location opposite to the laser welding. Evaluation of melt wires was accomplished by obtaining initial XCT images of a sealed melt wire assembly before the experiment to serve as a reference point. Then, after the experiment a new XCT image was obtained and compared against the reference image to determine if any melting had occurred. Tin was the lowest melting point material and had the most obvious changes compared to the other two printed materials. The XCT images of the zinc melt wire were not clearly defined; however, after adjusting contrast to optimize the XCT images, subtle changes could be identified to imply melting had occurred. For the evaluation of aluminum, the printed line on the original XCT image was unclear, and in the post-furnace image the aluminum wire was even harder to identify; therefore, confirmation of melting was considered inconclusive. Overall, results show a successful outcome in creating an inert gas encapsulation and high-resolution evaluation using XCT.

6. FUTURE WORK

As discussed in this report, multiple discoveries during design optimization of AM melt wires created more challenges that were not initially expected. The first focus for the future work will be broadening the material selection and geometries for the encapsulation, as we were unable to capture high-resolution XCT images and have a conclusive melting behavior of Al on SS substrate. This will enable AM melt wires to provide multiple material selection for encapsulation as well as guarantee high-resolution XCT images of PIE melting.

Additionally, it was possible that a very small amount of oxygen entered during an inert gas encapsulation that could have oxidized the Al to be unidentifiable post-melting in the XCT image. To further improve the encapsulation method, entrapping Helium required laser welding a weephole through a quartz window of an enclosed chamber where air could be purged and replaced with helium using a vacuum and having a weep hole machined for perfect one-shot weld.

Finally, the last focus of future work would be on the printed materials. Studying binder effects on material performance, determine effectiveness of oxygen getter additives, and design specific print patterns advantageous to specific material melting characteristics (pooling, surface tension collection, rounded edges, etc.) would greatly enhance the post-melting XCT images. Again, being able to broaden melt wire selection and how each material has its unique material characteristics could benefit the post-melting evaluation.

7. REFERENCES

1. P. Calderoni, D. Hurley, J. Daw, A. Fleming, and K. McCary, "Innovative sensing technologies for nuclear instrumentation," I2MTC 2019 - 2019 IEEE Int. Instrum. Meas. Technol. Conf. Proc., vol. 2019-May, 2019.
2. K. Bong Goo, J. L. Rempe, J. F. Villard, and S. Solstad, "Review of instrumentation for irradiation testing of nuclear fuels and materials," Nucl. Technol., vol. 176, no. 2, pp. 155–187, 2011.
3. Marshall, Frances M. *Advanced test reactor capabilities and future operating plans*. No. INL/CON-05-00549. Idaho National Laboratory (INL), 2005.
4. J. E. Daw et al., "Temperature monitoring options available at the Idaho national laboratory advanced test reactor," AIP Conf. Proc., vol. 1552 8, no. September, pp. 970–975, 2013.
5. K. L. Davis, D. L. Knudson, J. E. Daw, J. L. Rempe, and A. J. Palmer. 2012. "Melt Wire Sensors Available to Determine Peak Temperatures in ATR Irradiation Testing," Eighth American Nuclear Society International Topical Meeting on Nuclear Plant Instrumentation, Control. Human-Machine Interface Technology. Enabling the Future of Nuclear Energy. https://www.osti.gov/biblio/1054299-melt-wire-sensors-available-determine-peak-temperatures-atr-irradiation-testing.
6. T. Seifert, E. Sowade, F. Roscher, M. Wiemer, T. Gessner, and R. R. Baumann, "Additive manufacturing technologies compared: Morphology of deposits of silver ink using inkjet and aerosol jet printing," Ind. Eng. Chem. Res., vol. 54, no. 2, pp. 769–779, 2015.
7. K. Mondal, K. Fujimoto, and M. D. McMurtrey, "Advanced Manufacturing of Printed Melt Wire Chips for Cheap, Compact Passive In-Pile Temperature Sensors," Jom, vol. 72, no. 12, pp. 4196–4201, 2020.
8. K. Mondal, K. Fujimoto, and M. McMurtrey, "Non-visual analysis of miniaturized melt wire arrays for in-pile measurement of peak irradiation temperature," 2020.